

Combining dynamical mean-field theory and realistic band structure for V_2O_3

T. Wolenski, M. Grodzicki, and J. Appel
 Universität Hamburg, I. Institut für Theoretische Physik
 Jungiusstraße 9, D-20355 Hamburg.
 (November 23, 2018)

Recent neutron scattering experiments on V_2O_3 show that the magnetic fluctuations on the metallic side of the antiferromagnetic metal-insulator transition are not related to the spin structure of the insulator, but rather to the bandstructure-driven spin-density wave phase of the doped system $V_{2-y}O_3$. We calculate these magnetic fluctuations starting from a Slater-Koster bandstructure and incorporating the correlation effects through the dynamical mean-field theory (DMFT). Our results demonstrate that the magnetic properties of the paramagnetic metallic phase are dominated by the Fermi surface topology. On the other hand, the electron-electron interaction drives the paramagnetic metal-insulator transition in V_2O_3 . The transition to the antiferromagnetic insulator by virtue of orbital ordering is discussed in the framework of the DMFT.

Vanadium sesquioxide V_2O_3 is special among the many fascinating transition-metal oxides as it served as one of the first examples of a material exhibiting an interaction-driven Mott-Hubbard metal-insulator transition (MIT). The phase diagram of V_2O_3 (cf. Fig. 1 a) shows four different phases. The controlling variable, besides the temperature, is the ratio of local Coulomb interaction U and bandwidth D as evidenced by the similar response to substitutional doping with Cr and Ti or vanadium deficiency on the one hand and the application of hydrostatic pressure on the other hand. At low temperatures, an antiferromagnetic insulator (AFI) and an antiferromagnetic metal (AFM) occur. The spin structures of these magnetically ordered phases differ dramatically [1]. At higher temperatures, a first-order paramagnetic metal-insulator transition occurs, ending in a second-order critical point. The magnetic fluctuations in the paramagnetic phases have recently been shown to correspond to the long-range order observed in the AFM [2].

Experimentally, there are indications that the transition to the AFM phase is a spin-density wave transition, i.e. an electronic instability due to the formation of electron-hole pairs because the Fermi surface has nesting sheets: Parts of the Fermi-surface are almost parallel, providing large phase space of low-energy electron and hole excitations at positions \mathbf{k} and $\mathbf{k} + \mathbf{Q}$ in momentum space that are connected by the same nesting vector \mathbf{Q} . We recently demonstrated that this mechanism indeed provides an explanation for the properties of the AFM phase [3].

The point of departure is the electronic structure of V_2O_3 . Early attempts to calculate the bandstructure of V_2O_3 [4] were based on tight-binding calculations in a strongly reduced basis set, and are thus at best qualitatively correct. Recently, state-of-the-art density functional theory (DFT) results were made available [5]. To incorporate these results we employ the Slater-Koster method, which uses the DFT energy eigenvalues at points of high symmetry to parameterize tight-binding matrix

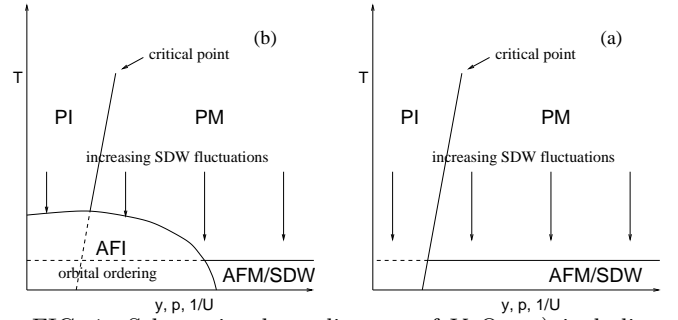


FIG. 1. Schematic phase diagram of V_2O_3 , a) including and b) without the orbital ordering transition to the AFI. Cf. text for abbreviations, Ref. [3] for numerical values.

elements, which can then be evaluated at any point in the Brillouin zone. This reduces the numerical effort to obtain reliable bandstructure information. Details of this approach are provided in a recent article [3].

Using this bandstructure we are able to calculate the properties of the SDW transition [3] within a weak-coupling Hartree-Fock mean-field theory, and find excellent agreement with the experimental situation [1,6]. The value of the Fermi surface nesting vector responsible for the spin-density wave instability is found to be $\mathbf{Q} = 1.69 c^*$, the transition temperature to be 10 K at an effective Hubbard interaction $U_c \simeq 0.5$ eV, in good agreement with optical experiments [7]. The success of the weak-coupling theory shows that the spin-density wave is Fermi-surface-driven, and is not a frustration phenomenon of the antiferromagnetic insulator as suggested previously [8,9]. The occurrence of the paramagnetic MIT on the other hand indicates that correlations are important in V_2O_3 .

The dynamical mean-field theory (DMFT) employed here is based on the insight that in the limit of high spatial dimensions or, better, for high lattice co-ordination spatial fluctuations become irrelevant, while dynamical quantum fluctuations remain important as shown by Vollhardt and Metzner [10]. This procedure allows to chose one lattice site $i = 0$ and integrate out all

other degrees of freedom, leading to a local effective action $S_{\text{eff}}[\mathcal{G}_0]$, which is a functional of an effective field $\mathcal{G}_0(\tau - \tau')$. The effective field describes the interaction of the local problem at $i = 0$ with a bath made up of the rest of the lattice. An electron at $i = 0$ can go into the bath at (imaginary) time τ and return to the local site at τ' . Excellent reviews of the DMFT include Ref. [11].

The solution of the local problem remains non-trivial. Here, we use the so-called modified iterated perturbation theory (MIPT), which becomes exact in both the weak coupling and atomic limit and at low and high frequencies [12]. The self-energy $\Sigma(i\omega_n)$ in MIPT is obtained through the Ansatz

$$\Sigma^{\text{MIPT}}(i\omega_n) = U \langle n \rangle + \frac{a\Sigma^{(2)}(i\omega_n)}{1 - b\Sigma^{(2)}(i\omega_n)}, \quad (1)$$

where $\Sigma^{(2)}(i\omega_n)$ is the second-order perturbation theory result,

$$\Sigma^{(2)}(i\omega_n) = U^2 \int_0^\beta d\tau e^{i\omega_n \tau} \mathcal{G}_0(\tau)^3. \quad (2)$$

Details on obtaining a and b to fit various limiting case are given in Ref. [12]. The lattice enters through a self-consistency condition: The effective field of the local problem is identified with the local Green's function of the lattice problem, and the full lattice Green's function $G(\mathbf{k}, i\omega_n)$ is calculated from the local self-energy. The self-consistency equation is

$$\Sigma(i\omega_n) = \mathcal{G}_0^{-1}(i\omega_n) - G^{-1}(i\omega_n) \quad (3)$$

and

$$G(i\omega_n) = \sum_{\mathbf{k}} G_{\mathbf{k}}(i\omega_n) = \sum_{\mathbf{k}} \frac{1}{i\omega_n - \epsilon_{\mathbf{k}} + \mu - \Sigma(i\omega_n)}. \quad (4)$$

The momentum summation brings in the density of states of the actual lattice. Before employing the MIPT, we point out that Rozenberg *et al.* [9] applied the DMFT on a Bethe lattice to get a fairly complete picture of the interaction-driven metal-insulator transition, where they introduce phenomenological frustration to suppress a Slater-type transition. A first central point here is that we show that their results regarding the paramagnetic MIT essentially carry over to the case of V_2O_3 including the realistic bandstructure as presented in Ref. [3].

In Fig. 2 we show the development of the spectral function $A(\omega) = -1/\pi G(\omega + i0^+)$ as the interaction U is tuned through the MIT. It is obtained after solving the DMFT in the MIPT approximation and Padé-transforming the results to the real frequency axis. The transfer of spectral weight to higher frequencies and the eventual formation of upper and lower Hubbard bands is clearly seen. As long as the system stays metallic $A(0)$ does not change, as required for a local self-energy. The narrowing of the quasi-particle peak at $\omega = 0$ can be

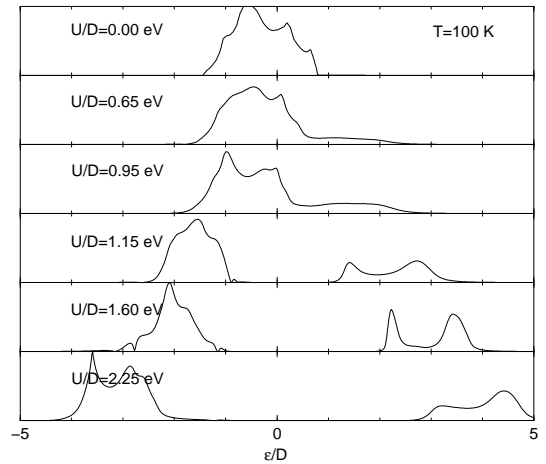


FIG. 2. Development of the spectral function as the interaction U is tuned through the MIT.

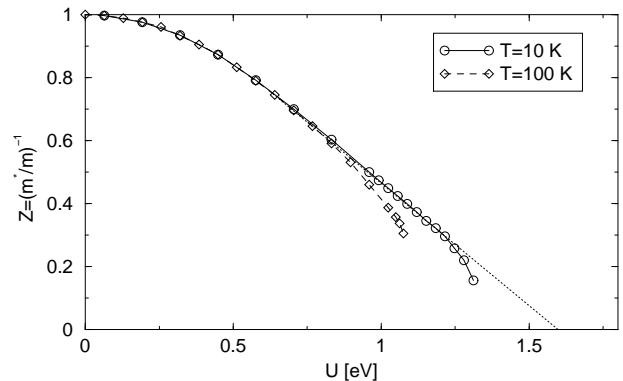


FIG. 3. Divergence of the effective mass m^* at the MIT. Dotted line is an extrapolation to $T = 0$.

described as a divergence of the effective mass m^* or reduction of the quasiparticle weight Z , given by

$$\frac{m^*}{m} = \frac{1}{Z} = 1 - \frac{\partial}{\partial \omega} \text{Re } \Sigma(\omega + i0^+) \Big|_{\omega=0}. \quad (5)$$

The result is shown in Fig. 3. The finite temperature curves extrapolate to a linear behavior at $T = 0$.

Rozenberg *et al.* found a coexistence regime for metallic and insulating solutions of the DMFT equations. We confirmed this finding for the realistic bandstructure of V_2O_3 . Fig. 4 shows the stability regimes, the metallic solution is stable for $U < U_{c2}$, the insulating solution for $U > U_{c1}$. The physical phase transition occurs at the crossing of the free energy surfaces of these curves, indicated by the dashed line in Fig. 4. The dotted line is an extrapolation of U_{c2} to $T = 0$ based on Fig. 3. The values of the transition temperatures and the effective interaction agree well with experimental values [7].

While the consideration of the realistic bandstructure did only provide quantitative corrections of the paramagnetic MIT, it is essential for obtaining even a qualitative picture of the magnetic properties. Rozenberg *et al.* extended their study to include frustrated magnetism in

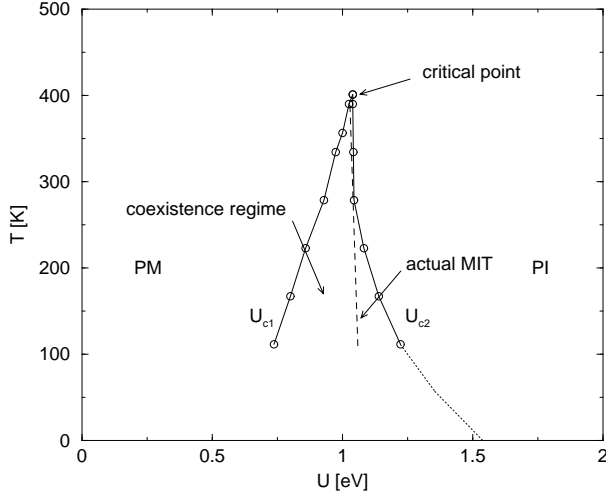


FIG. 4. Stability regime of metallic and insulating solutions to the DMFT equations. Dashed line indicates physical phase transition.

the Bethe lattice, but this approach is not able to explain the different spin structures of the AFI and AFM and the absence of any AFI-type fluctuation in the PM in close proximity to the AFI [2].

Since the magnetic structure of the AFM phase and the corresponding fluctuations in the paramagnetic phases are experimentally known to be incommensurate, the only way to study them is through the dynamic spin susceptibility, as no precursors of a symmetry breaking phase can be seen on the one-particle level as $d \rightarrow \infty$ [13]. The DMFT is used here as an approximation to calculate the momentum dependent susceptibility; it is determined by the lattice Green's functions, Eq. (4), as

$$\chi^0(\mathbf{q}, \omega) = - \sum_{\mathbf{k}, \nu} G(\mathbf{k}, \nu) G(\mathbf{k} + \mathbf{q}, \omega + \nu). \quad (6)$$

The full susceptibility χ is obtained from χ^0 after the vertex functions are taken into account [11], which become momentum independent as $d \rightarrow \infty$.

The dynamic susceptibility is connected with the neutron scattering intensity through the fluctuation-dissipation theorem, which allows the comparison with the measurements of Bao *et al.* [2,14]. We present three characteristic points in the PM phase: A is chosen close to the paramagnetic MIT and close to the AFI, B and C are at different temperatures above the AFM low-temperature phase. In Fig. 5 we show the momentum dependence of the susceptibility for a given small frequency ω . At all temperatures the maximum in the susceptibility is at the wave vector \mathbf{Q} corresponding to the AFM spin-density wave structure. Remarkably, at A no evidence of the close AFI phase is seen, in agreement with neutron scattering results. The comparison of B and C shows the increase of the intensity at \mathbf{Q} as the spin-density wave transition is approached.

In Fig. 6 the frequency dependence of $\chi(\mathbf{q} = \mathbf{Q}, \omega)$ is

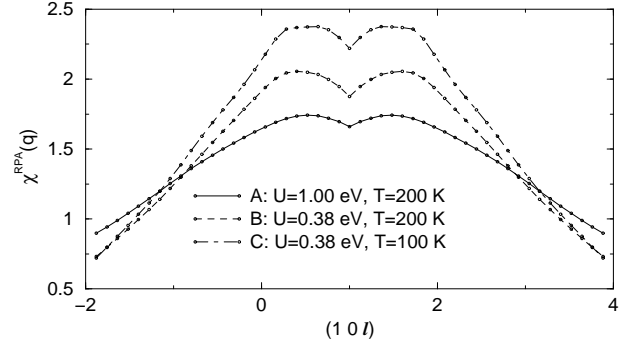


FIG. 5. Dynamic susceptibility at different points in the phase diagram (cf. text). The wave vector at the maximum of $\chi(\mathbf{q}, \omega)$ corresponds to the long-range order observed in the AFM.

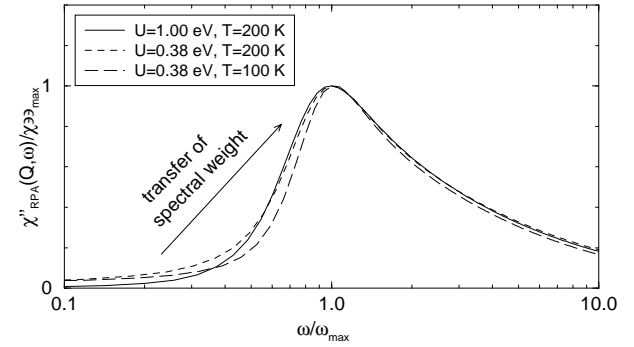


FIG. 6. Frequency dependence of the dynamic susceptibility at the same parameter values as in Fig. 5.

shown, scaled approximately on a single curve. This is to be compared with the results of Bao *et al.* [14]. Bao *et al.* fit their results with the SCR theory for itinerant antiferromagnetism [15]. Our curve has spectral weight transferred to higher frequencies compared to the SCR due to the strong correlations, and does improve on the fit to the experimental result.

We demonstrate that the combination of the DMFT with the realistic bandstructure provides a natural description of the paramagnetic metal-insulator transition, the spin-density wave transition, and the magnetic fluctuations of the paramagnetic phases. This is summarized in Fig. 1 b). In particular, this parameter-free calculation gives good quantitative agreement with experimental results, both for the spin-density wave [3] and the MIT. The absence of any AFI-type fluctuations outside the AFI as observed in neutron scattering experiments is due to the strongly first order transition to the AFI.

Let us now turn to the AFI. Castellani *et al.* [16] suggested several years ago, that the essential mechanism of the AFI is orbital ordering [17]. In V_2O_3 , the vanadium e_g orbitals form a doubly degenerate, quarter-filled band. The degeneracy is lifted in second-order perturbation theory, leading to a favoring of ferromagnetic spin and “antiferromagnetic orbital” coupling, i.e. a staggered occupation of the two degenerate orbitals.

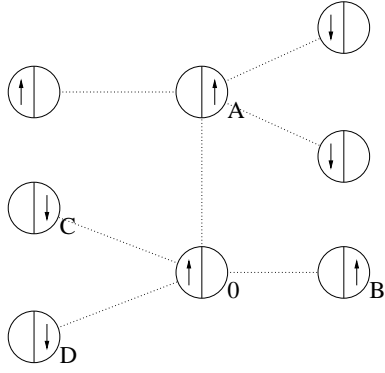


FIG. 7. Proposed cluster of vanadium sites to study orbital ordering in the AFI of V_2O_3 . The split circles denote the occupation of the two degenerate orbitals at each site [16,17].

Castellani *et al.* were able to apply this idea to V_2O_3 and demonstrate that the observed spin structure of the AFI can be explained in this approach. It is thus necessary to go beyond the effective one-band model studied so far [3].

While this complements our picture of V_2O_3 , the approach of Castellani has two shortcomings from today's point of view: The authors had to rely on the band-structure calculations available at the time [4] and strong correlations have not been taken into account, even in a regime where the paramagnetic MIT is known to occur. These corrections are not expected to be essential, yet for a complete picture of V_2O_3 it is desirable to include them in the calculation. To that end, the DMFT equations have to be generalized to a cluster of vanadium sites as shown in Fig. 7. This approach is similar to introducing two sublattices to study simple AB-type antiferromagnetism. Here, four neighbor sites of $i = 0$ have to be considered. The Green's functions for these sites are related by

$$G_{\nu\sigma}^0 = G_{\nu\sigma}^A = G_{\nu\sigma}^B = G_{\nu\sigma}^C = G_{\nu\sigma}^D \quad (7)$$

where ν is an orbital index and we suppressed the argument $i\omega_n$. The orbitally dependent DMFT equations have been derived by Momoi and Kubo and by Held and Vollhardt [18] for the doubly-degenerate Hubbard model. The hopping matrix elements $t_{ij}^{\nu\nu'}$ and the eigenvectors $A_{\nu\alpha}(\mathbf{k})$, where α is a band index, can be obtained from the bandstructure calculation. One has

$$t_{ij}^{\nu\nu'} = \sum_{\mathbf{k}} e^{i\mathbf{k} \cdot (\mathbf{R}_i - \mathbf{R}_j)} \sum_{\alpha} A_{\alpha\nu}(\mathbf{k}) \epsilon_{\mathbf{k}}^{\alpha} A_{\alpha\nu'}^*(\mathbf{k}). \quad (8)$$

To solve the coupled problem is straightforward in principle but has not yet been performed for V_2O_3 .

In conclusion, the various phase transitions of V_2O_3 are consistently explained once the physics of strong correlation and the realistic bandstructure are combined. Apart from the calculation of orbital ordering within DMFT, some other open questions remain. A systematic $1/d$ -expansion would complement the assumption of

high spatial dimensions in the treatment of the strong-correlation problem. The importance of disorder, which is certainly present at least in the doped V_2O_3 compounds, has not been studied. Dobrosavlević and Kotliar [19] provided a promising extension of the DMFT to the dirty limit. And, finally, the absence of superconductivity in V_2O_3 is still a challenging problem. The solution to this last problem promises new insights into the basic mechanism of high-temperature superconductivity in the cuprates. One possible scenario is that the large local moments known to occur in metallic $V_{2-y}O_3$ [6] destroy the superconductivity, so that it would be interesting to look for superconductivity in completely stoichiometric V_2O_3 , where the metallic phase has been stabilized through application of hydrostatic pressure.

T. W. acknowledges financial support from the Universität Hamburg; this work is in partial fulfillment of his doctoral degree at this university.

-
- [1] W. Bao *et al.*, *Phys. Rev. Lett.* **71**, 766 (1993).
 - [2] W. Bao *et al.*, *Phys. Rev. B* **54**, R3726 (1996); W. Bao *et al.*, *Phys. Rev. Lett.* **78**, 507 (1997).
 - [3] T. Wolenski, M. Grodzicki, and J. Appel, *Phys. Rev. B* **58**, 303 (1998).
 - [4] I. Nebenzahl and M. Weger, *Phil. Mag.* **24**, 1119 (1971); J. Ashkenazi and T. Chuchem, *Phil. Mag.* **32**, 763 (1975).
 - [5] L. F. Mattheiss, *J. Phys.: Condens. Matter* **6**, 6477 (1994); M. Grodzicki and O. Jepsen, unpublished.
 - [6] S. Langenbuch, M. W. Pieper, P. Metcalf, and J. M. Honig, *Phys. Rev. B* **53**, R472 (1996).
 - [7] G. A. Thomas *et al.*, *Phys. Rev. Lett.* **73**, 1529 (1994).
 - [8] S. Sachdev and A. Georges, *Phys. Rev. B* **52**, 9520 (1995).
 - [9] M. J. Rozenberg, X. Y. Zhang, and G. Kotliar, *Phys. Rev. Lett.* **69**, 1236 (1992); M. J. Rozenberg, G. Kotliar, and X. Y. Zhang, *Phys. Rev. B* **49**, 10181 (1994).
 - [10] W. Metzner and D. Vollhardt, *Phys. Rev. Lett.* **62**, 324 (1989); W. Metzner, *Phys. Rev. B* **43**, 8549 (1991).
 - [11] A. Georges, G. Kotliar, W. Krauth, and M. J. Rozenberg, *Rev. Mod. Phys.* **68**, 13 (1996); D. Vollhardt, in "Correlated Electron Systems," Ed. V. J. Emery, World Scientific, Singapore, 1993.
 - [12] H. Kajueter and G. Kotliar, *Phys. Rev. Lett.* **77**, 131 (1996); M. Potthoff, T. Wegner, and W. Nolting, *Phys. Rev. B* **55**, 16132 (1997).
 - [13] E. Müller-Hartmann, *Z. Phys. B* **76**, 211 (1989).
 - [14] W. Bao *et al.*, *Phys. Rev. B* **58** (19) (1998), cond-mat/9804320.
 - [15] K. Nakayama and T. Moriya, *J. Phys. Soc. Jap.* **56**, 2918 (1987).
 - [16] C. Castellani, C.R. Natoli, and J. Ranninger, *Phys. Rev. B* **18**, 4945 (1978); *ibid.*, *Phys. Rev. B* **18**, 4967 (1978).
 - [17] K.I. Kugel and D.I. Khomskii, *Sov.-Phys. JETP* **37**, 725 (1973); *Sov.-Phys. Usp.* **25**, 231 (1982); M. Cyrot and C. Lyon-Caen, *J. Physique* **36**, 253 (1975).
 - [18] T. Momoi and K. Kubo, *Phys. Rev. B* **58**, R567 (1998); K. Held and D. Vollhardt, cond-mat/9803182.
 - [19] V. Dobrosavlević and G. Kotliar, *Phys. Rev. Lett.* **78**, 3943 (1997); cond-mat/9706231.